



Tanshinone IIA promotes apoptosis by downregulating BCL2 and upregulating TP53 in triple-negative breast cancer

Jinfeng Liu¹ · Chang Zhang² · Shuang Liu¹ · Xiaokang Wang³ · Xiongzhī Wu⁴ · Jian Hao⁵

Received: 17 July 2022 / Accepted: 24 October 2022 / Published online: 14 November 2022
© The Author(s), under exclusive licence to Springer-Verlag GmbH Germany, part of Springer Nature 2022

Abstract

Tanshinone IIA (Tan IIA) was mainly used for cardiovascular disease treatment. Recent studies have demonstrated the role of Tan IIA for tumor treatment, but its mechanism remains unclear. At the first, the inhibitory effect of Tan IIA on 4T1 breast cancer cells was determined by CCK8 and colony formation assay. Then, a 4T1 BALB/c model of breast cancer was established to evaluate the anti-cancer effect of Tan IIA *in vivo*. Flow cytometry analysis and the TUNEL test were used to detect cell apoptosis *in vitro* and *in vivo*, respectively. The related targets and mechanisms of Tan IIA were predicted through network-based systems biology. At last, molecular docking and the molecular biological techniques were used to evaluate the predicted targets. Tan IIA displayed encouraging inhibitory influences on 4T1 cells after incubation for 24 h and showed a half-maximal inhibitory concentration (IC50) of 49.78 μM after 48-h incubation. After 23 days of treatment, the relative tumor volumes in the Tan IIA group were 65.53% inhibited compared with the control group. Furthermore, Tan IIA induced 4T1 cell apoptosis both *in vivo* and *in vitro*. The possible targets of Tan IIA for TNBC treatment were predicted with network-based systems biology, and results showed that TP53, NF-κB, AKT, MYC, and BCL-2 were the hub targets. The mechanism against breast cancer may be based on the P53 signaling pathway, the PI3K/Akt pathway, the MAPK signaling pathway, and the mTOR signaling pathways. Molecular docking analysis reveals that Tan IIA has a high affinity for p53, Bcl-2, and NF-κB1; the binding energies were –6.92, –6.07, and –6.28 kcal/mol, respectively. The predicted proteins were further validated using Western blotting. Increased expression of phosphorylated p53 and p53 and decreased expression of Bcl-2 were found in Tan IIA-treated 4T1 cells. Tan IIA is potentially effective for the treatment of 4T1 breast cancer, and the molecular mechanism may be through enhancing the activity of p53 and decreasing Bcl-2 to suppress proliferation and promote apoptosis.

Keywords Tanshinone IIA · Triple-negative breast cancer · Apoptosis · Network pharmacology · TP53 · BCL2

Introduction

Breast cancer is the malignant tumor with the highest incidence rate among women all over the world (Sung et al. 2021). Triple-negative breast cancer (TNBC) is the subgroup

Jinfeng Liu, Chang Zhang, and Shuang Liu have contributed equally to this study and share first authorship.

✉ Xiongzhī Wu
wuxiongzhī@163.com

✉ Jian Hao
bingxin@tmu.edu.cn

¹ Key Laboratory of Cancer Prevention and Therapy, Tianjin Medical University Cancer Institute and Hospital, National Clinical Research Center for Cancer, Tianjin's Clinical Research Center for China, Tianjin 300060, China

² Department of Traditional Chinese Medicine, General Hospital of Pingmei Shenma Group, Pingdingshan 467000, China

³ Department of General Surgery, Shanghai General Hospital, Shanghai Jiao Tong University School of Medicine, Shanghai 200086, China

⁴ Oncology Research Center of Integrated Traditional Chinese and Western Medicine, Tianjin Medical University Nankai Hospital, Nankai District, Changjiang Road, Tianjin 300102, China

⁵ Department of Rheumatism and Immunology, Tianjin Medical University General Hospital, An-Shan Road, Heping District, Tianjin 300052, China

lacking ER, PR, and HER2 expression. It accounts for 15% of total breast cancer patients with a high biological aggressive nature and a high rate of proliferation and invasion (Waks and Winer 2019; Arnedos et al. 2012). Despite the improvement of treatment strategies, the prognosis of TNBC patients remains poor. Searching for effective regimens remains the top priority in TNBC research.

As one of the herbs with a long history of application, danshen (*Salvia miltiorrhiza*) is widely used in cardiovascular diseases. Tanshinone, one of the main lipophilic components of *Salvia miltiorrhiza*, has been proved to have diverse pharmacological activities including anti-inflammation, anti-oxidation, and anti-cancer. Tanshinone IIA (C₁₉H₁₈O₃, Tan IIA, Fig. 1) is one of the important tanshinones. For the well-reported anti-inflammatory and antiangiogenic activities, the antitumor effects of Tan IIA have received more attention in gastric cancer, colorectal cancer, lung cancer, etc. (Sui et al. 2017; Xu et al. 2018; Wang et al. 2019; Li et al. 2020 Apr). The anti-TNBC effects of Tan IIA have been reported (Wu et al. 2018), but the mechanisms are currently unclear.

Network pharmacology, a new discipline of multi-target drug molecular design, reveals the synergistic effect of Chinese herbal medicine on diseases and its underlying mechanism by constructing a multi-component and multi-target network (Hopkins 2008; Hao and Li 2018; Xian et al. 2021). The aim of the present study was to investigate the effects and mechanisms of Tan IIA on the TNBC treatment. We found that Tan IIA is potentially effective for the treatment of 4T1 breast cancer, and the molecular mechanism may be through enhancing the activity of p53 and decreasing Bcl-2 to suppress proliferation and promote apoptosis.

Materials and methods

Drugs and reagents

Tan IIA (purity: 99.35%, Fig. 1) was purchased from Chengdu Mansite Biotech Co. Ltd (China, Lot. MUST-19090910). Doxorubicin (Dox) was obtained from Beijing Solarbio Science & Technology Co., Ltd. (China, Lot. 730M024). Cell Counting Kit-8 was purchased from MedChemExpress (USA, Lot. #67,666). Antibodies against Bcl-2 (ab79849), P53 (ab26), phospho-P53(ab33889), and β-actin (ab8226) were purchased from Abcam (UK).

Cell lines and cultures

Murine triple-negative breast cancer 4T1 cell lines and the normal breast cell line (MCF10A) were kindly provided by Procell Life Science & Technology Co., Ltd. Due to the

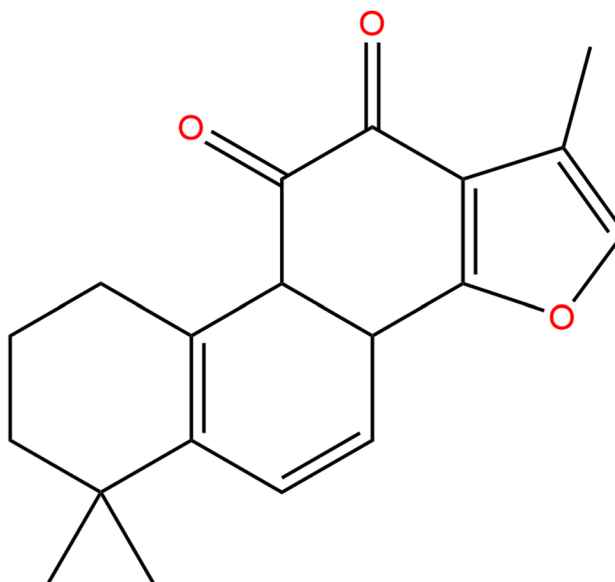


Fig. 1 The molecular structure of Tanshinone IIA

growth and metastatic properties, tumor-bearing mice with 4T1 cells are an animal model of human stage VI breast cancer. 4T1 cells were expanded in a humidified incubator at 37 °C with 5% CO₂ in RPMI-1640 medium (Gibco, USA), supplemented with 100 U/mL penicillin (Gibco, USA) and 100 mg/mL streptomycin (Gibco, USA) and 10% fetal bovine serum (Gibco, USA). MCF10A cells were cultured in DMEM medium (Gibco, USA) supplemented with 10 µg/mL insulin (Thermo Fisher Scientific, USA), 20 ng/mL human epidermal growth factor (HEGF) (Thermo Fisher Scientific, USA), 0.5 µg/mL hydrocortisone (Thermo Fisher Scientific, USA), 5% horse serum (Thermo Fisher Scientific, USA), and 5% penicillin–streptomycin (Gibco, USA). The cells were also incubated in a humidified incubator with 5% CO₂ under 37 °C.

Cell proliferation assay

CCK-8 viability assay was performed to evaluate the effects of Tan IIA on cell proliferation. For this, 4T1 and MCF10A cells, suspended with 0.25% trypsin (Gibco, USA), were inoculated into 96-well plates at a density of 3×10^3 cells per well. Subsequently, 4T1 cells were treated with Tan IIA at concentrations of 10, 20, 30, 40, 50, 60, 70, or 80 µM for 24, 48, and 72 h, respectively. And MCF10A cells were treated with the highest concentration of Tan IIA (80 µM). Finally, 96-well plates incubated with 10 µL of CCK-8 solution for 60 min were detected by a microplate reader (IMark, Bio-Rad). Record the absorbance (Abs) at 450 nm and calculate the cell inhibition rate (Xue et al. 2019). All experiments were performed in six replicates and repeated three times.

Colony formation assay

Transfected cells were reseeded into 6-well plate with 500 cells per well by treating with Tan IIA for 48 h. Cells were further treated with 0 (DMSO), 12.5, 25, or 50 μ M Tan IIA, and 3 wells were used per group. Then, 6-well plates cultivated at 37 °C for approximately 12 days were washed with 1×PBS and fixed with 4% paraformaldehyde for 30 min at room temperature. Finally, natural colonies stained with 0.5% crystal violet for approximately 20 min were imaged and quantified. All experiments were performed in triplicate and repeated three times.

Apoptosis assay by flow cytometry

The Fluorescein Isothiocyanate (FITC) Annexin V Apoptosis Detection Kit I (BD Pharmingen, USA) was used to detect apoptotic cells following the manufacturer's protocol. 4T1 cells were treated with Tan IIA in serial concentrations (0, 12.5, 25, and 50 μ M) at 37 °C for 24 h. After washing with PBS, cells were trypsinized and subsequently incubated in FITC-conjugated Annexin-V binding buffer containing PI in the dark for 15 min. After incubation, cell apoptosis was assessed using FCS Express software (De Novo Software) on EXFLOW (Dakewe Biotech Co., Ltd.).

Network pharmacology analysis

As in our previous researches (Liu et al. 2021), the possible targets of Tan IIA were predicted from the following two databases: BATMAN-TCM (Liu et al. 2016) (<http://bionet.ncpsb.org.cn/batman-tcm/>) and TCMSP Database and Analysis Platform (Jinlong et al. 2014) (<https://tcmsp.com/tcmsp.php>). Candidate TNBC targets were obtained from CTD (Davis et al. 2020) (<http://ctdbase.org/>) and TTD databases (Wang et al. 2020) (<http://db.idrblab.net/ttd/>). Analyze the function of predicted targets based on the DAVID bioinformatics database (Davis et al. 2017). Protein–protein interactions (PPI) were constructed with Cytoscape based on the STRING database (Szklarczyk et al. 2014).

Docking exercises of ingredients binding to main targets

Compound structures were obtained from TCMSP Database and Analysis Platform and saved as docking ligands in MOL2 format. The crystal structure of p53, Bcl-2, and NF- κ B1 was obtained from the Protein Data Bank (PDB ID: 3D06 (Suad et al. 2009), PDB ID: 6GL8 (Casara et al. 2018), and PDB ID: 1MDI (Qin et al. 1995)). Other targets' crystal structures from Protein Data Bank include EGFR (5UG9), CASP3 (4JJE), KIT (3G0E), AKT2 (1O6L), and Bcl-2l1 (3SP7) (Planken et al. 2017; Vickers

et al. 2013; Gajiwala et al. 2009; Yang et al. 2002; Zhou et al. 2012). The crystal structures of candidate proteins were modified using the Autodock 4.2 software (Morris et al. 2009) to remove ligands, add hydrogen, remove water, and patch amino acids. The docking binding free energy was scored, and the docking models with the lowest binding affinity were displayed by PyMOL (3D).

Western blotting

Total protein from Tan IIA-treated cell lysis was quantified according to the manufacturer's BCA protein guideline, separated on 10% SDS-PAGE, and transferred to PVDF membranes. After blocking with 5% defatted milk dissolved in Tris-buffered saline containing 0.1% Tween-20, membranes were incubated with appropriate dilutions of primary antibodies (BCL2, TP53, phosphor-TP53, and β -actin (Abcam, Cambridge, UK)) followed by secondary antibody. Finally, quantification was performed using an image acquisition and analysis system (CHEMIDOC XRS +, Bio-Rad, USA) and ImageJ (Su 2018).

In vivo xenografts

2×10^6 4T1 cells were injected subcutaneously into the upper middle groin of 5 BALB/c female mice. Tumor volumes were determined every day (tumor volume = length*width²/2). When the average length of the subcutaneous tumor reached 10 mm, the mice were sacrificed in a humane manner, and then the tumors were collected. The collected tumors were cut into small pieces with a length of 2 mm in the clean area and planted in the fat pads of the fourth pair of left breasts of the anesthetized (Isoflurane, Rodent Anesthesia Machine, provided by Hebei Lanmeng Bio Pharmaceutical Technology Co., Ltd.) BALB/c female mice. Three days later, the mice were randomly divided into 3 groups ($n = 18$) and injected intraperitoneally every other day. The dosage was 2 mg/kg, the dosage of Tan IIA was 10 mg/kg (Lin et al. 2013), and the control group was given the same amount of normal saline. Starting from the 8th day, three mice were randomly selected from each group every 3 days and sacrificed in a humane manner. The tumors of the mice were isolated and stored at low temperature. All experiments were approved by the Experimental Animal Ethics Committee of Nankai University.

Immunohistochemistry (IHC) and TUNEL assay

After fixation and permeabilization, immunohistochemical sections of tumor tissue were prepared according to the

instructions of the KI67 Cell Proliferation Kit (IHC) (Sangon Biotech (Shanghai) Co., Ltd., China) to check the proliferation status. In addition, apoptosis in tumor tissues was detected using the In Situ Cell Death Detection Kit (Roche Diagnostic Mannheim, Germany) according to the manufacturer's instructions. Representative images were obtained using a confocal microscope (Olympus) (Hao et al. 2018) after the final overlay with DAPI-containing mounting medium.

Statistical analysis

Statistical significance was determined using SPSS 12.0. All experimental data were analyzed by one-way analysis of variance (ANOVA) with the Bonferroni correction for multiple comparisons.

Results

Effect of Tan IIA treatment on the proliferation of TNBC 4T1 cells

The effects of Tan IIA on the viability of 4T1 were evaluated with CCK-8 assay. 4T1 cells were exposed to various concentrations (10, 20, 30, 40, 50, 60, 70, or 80 μ M) of Tan IIA for 24, 48, and 72 h, respectively. When treated with more than 40 μ M of Tan IIA for 24 h, sustainable and stability-inhibitory effects were shown (Fig. 2A, B). Tan IIA inhibited 4T1 cell proliferation in concentration- and time-dependent manners as the IC₅₀ values at 24, 48, and 72 h were of 81.89, 49.78, and 41.60 μ mol/L, respectively. Moreover, Tan IIA had no obvious toxicity to normal breast cells ($P > 0.05$, Fig. 2A). Due to the specificity of 4T1 cells, we chose the IC₅₀ concentration via calculating at 48 h as the highest dose concentration for subsequent *in vitro* experiments (Fig. 2C).

Next, we determined the effect of Tan IIA on the ability of 4T1 to form colonies. Similarly, Tan IIA significantly reduced the colony formation by 67.73%, 31.87%, and 13.94% after treated with 12.5 μ M, 25 μ M, and 50 μ M of Tan II for 48 h (Fig. 2D). The underlying mechanism of cell viability inhibition was further studied by determining the apoptotic effects using the Annexin-V/PI method. The apoptotic cells (D2 + D3) increased after treated with Tan II with a concentration-dependent manner ($P < 0.01$, Fig. 2E). Consistent with the cell viability assays, these results again indicated the ability of Tan II to induce growth inhibition.

Effects of Tan II on xenograft tumor models

To further evaluate the anti-tumor efficacy of Tan IIA, BALB/C mice bearing 4T1 tumor were treated orally with

Tan IIA. Doxorubicin (Dox) was used for positive control. After the 23 days of treatment, no death or adverse events occurred in all groups. No significant differences in body weight change were observed in the three groups. Treatment with Tan II and Dox induced significant growth delay of 4T1 tumor compared to untreated controls, as shown in Fig. 3A. The tumor weight was reduced by 34.47% and 51.00% in Tan II-treated and Dox-treated groups, respectively. On the 23rd day, the relative tumor volumes of Tan IIA and Dox were 877.67 ± 250.80 mm³ and 656.33 ± 187.35 mm³, while the tumor volume of the control group was 1339.33 ± 56.58 mm³ (Fig. 3B).

Ki-67 expression analysis was performed to evaluate cell proliferation by immunohistochemistry. On the 23rd day, all the three groups showed Ki-67 strong staining. Ki-67 staining in the treated groups showed slightly weakened ($P < 0.05$, Fig. 3D). Apoptosis levels *in situ* were analyzed by the TUNEL assay, and the distribution of the TUNEL-positive nuclei was higher after the treatment of Tan IIA ($P < 0.05$, Fig. 3E).

Predicted targets and mechanisms of Tan IIA for breast cancer treatment based on network pharmacology

After searching the TTD and CTD databases, we obtained 1344 TNBC-related target candidates. Furthermore, 215 drug targets were predicted from BATMAN-TCM and TCMSP databases. The potential TNBC targets for Tan IIA treatment were matched by combining the disease and drug targets. Forty-five common targets were obtained to construct an ingredient-target (cI-cT) network using Cytoscape (Fig. 4A). We further put the screened 45 targets into the STRING website to get the protein–protein interactions (PPI) among these proteins with the conditional effect score that was set as > 0.9 . After removing the targets without interactions, a PPI with 39 targets was obtained (Fig. 4B), which indicated that these targets tend to form close associates among each other. TP53, NF- κ B, AKT, MYC, and BCL2 were the hub targets among the PPI network. The functions of 39 hub targets were further analyzed with the DAVID website; we found these targets majorly involved in cancer-related biological processes and pathways, such as cell apoptosis, P53 signaling pathway, PI3K/Akt pathway, the MAPK signaling pathway, and the mTOR signaling pathway (Fig. 4C, D).

To ascertain the interaction between Tan IIA and their hub targets, computational docking exercises were conducted to mimic the binding characteristics. It is generally believed that the binding energy value less than -5.0 kcal/mol indicates good binding activity, and less than -7.0 kcal/mol indicates strong binding activity. The binding energies of Tan IIA with these hub targets P53,

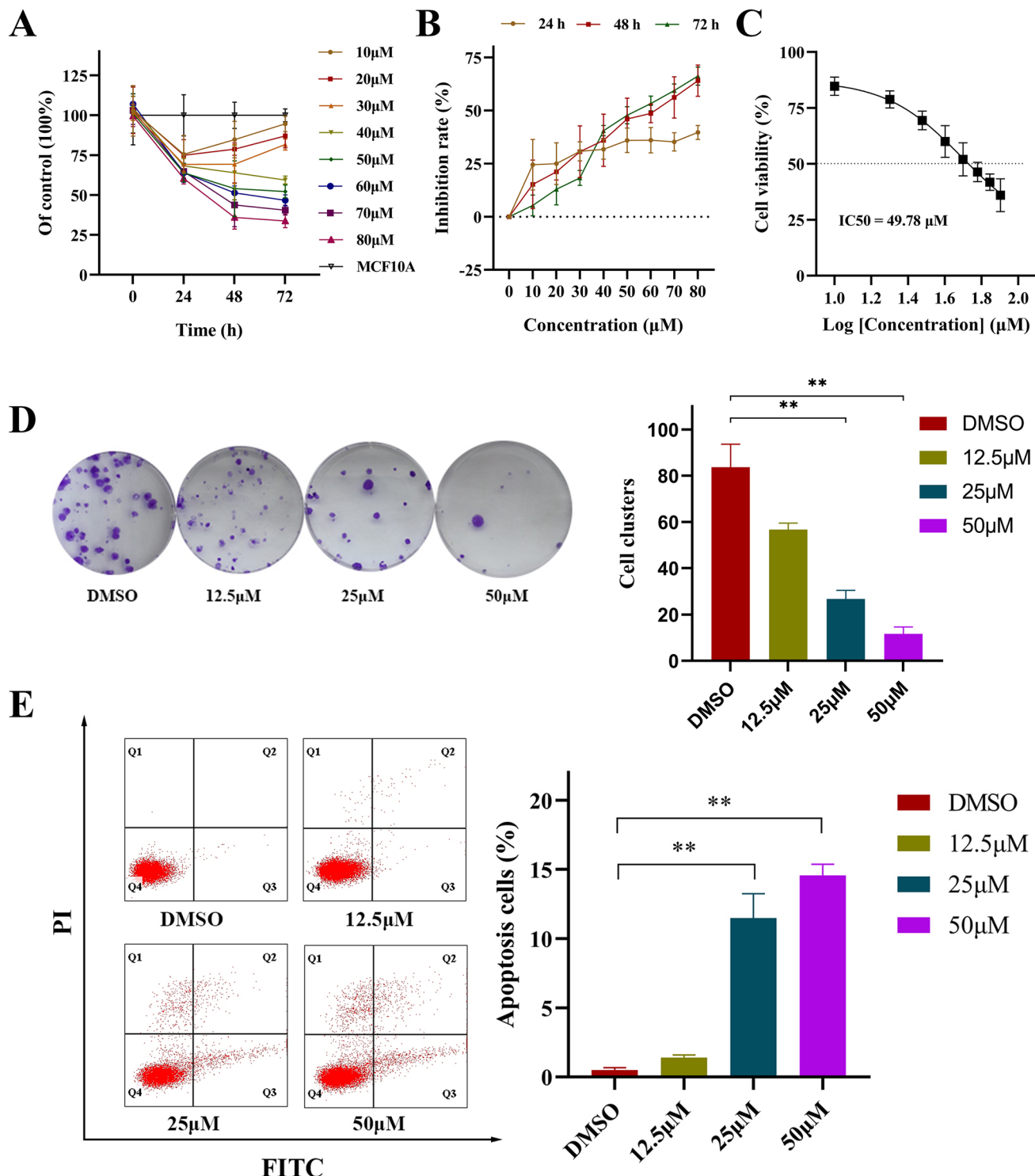


Fig. 2 The effect of Tan IIA treatment on the proliferation of TNBC 4T1 cells. **A, B** The effect of Tan IIA treatment on the proliferation of TNBC 4T1 cells and normal breast cells MCF10A. **C** The con-

centration-suppression rate curve of 48 h. **D** The plate clone formation assay. **E** Apoptotic effects of Tan IIA using the Annexin-V/PI method. ** $P < 0.01$

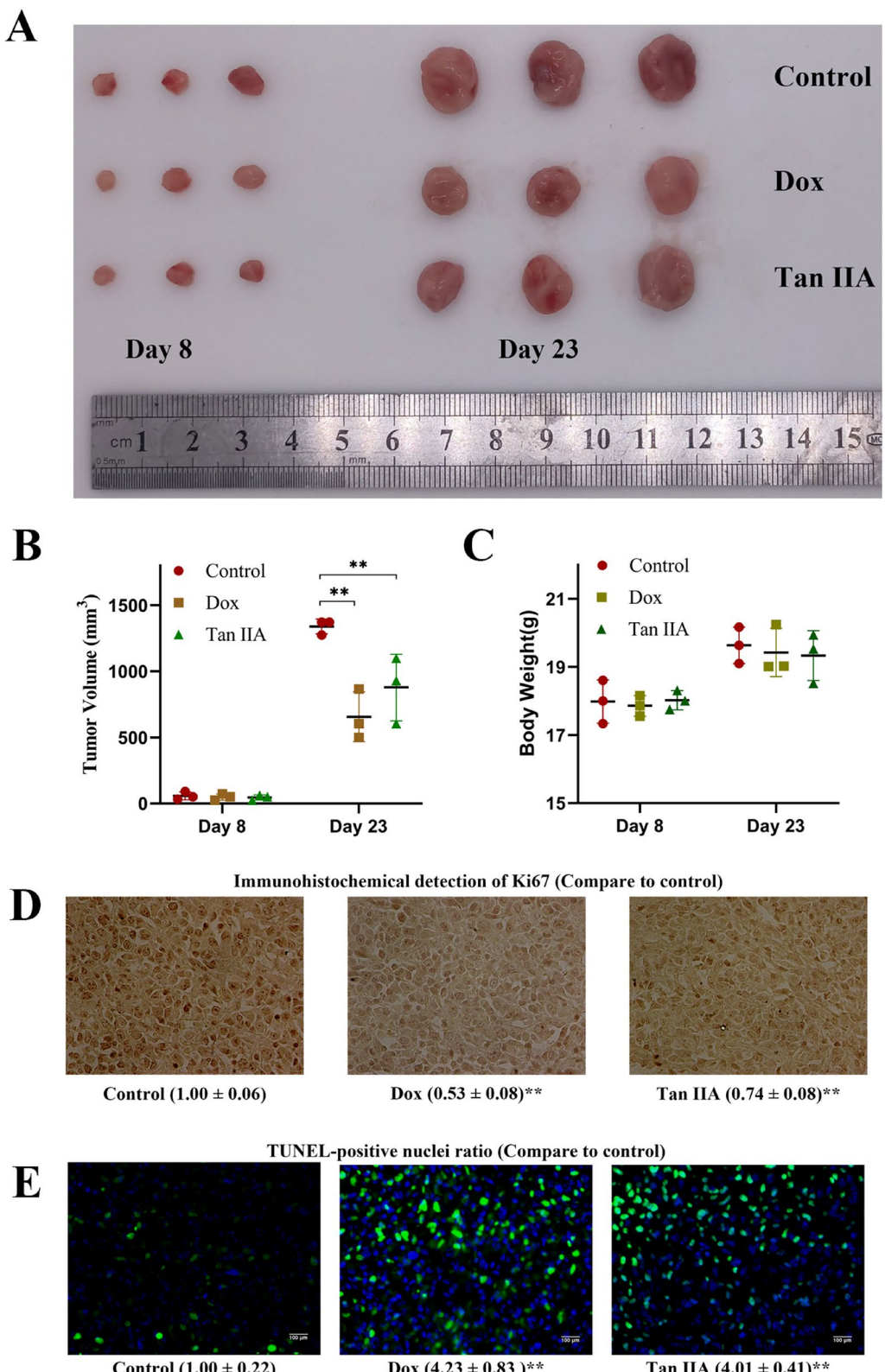


Fig. 3 In vitro experiments of tanshinone IIA. **A, B** Tan IIA suppresses tumor growth in vivo and the analysis of tumor volume. **C** Changes in weight of tumor-bearing mice. **D, E** Immunohistochemistry and TUNEL assay on tumor tissues of tumor-bearing mice (the distribution of the TUNEL-positive nuclei was higher after the treatment of Tan IIA compared to that in the control group, 100 \times). ** $P < 0.01$

tribution of the TUNEL-positive nuclei was higher after the treatment of Tan IIA compared to that in the control group, 100 \times). ** $P < 0.01$

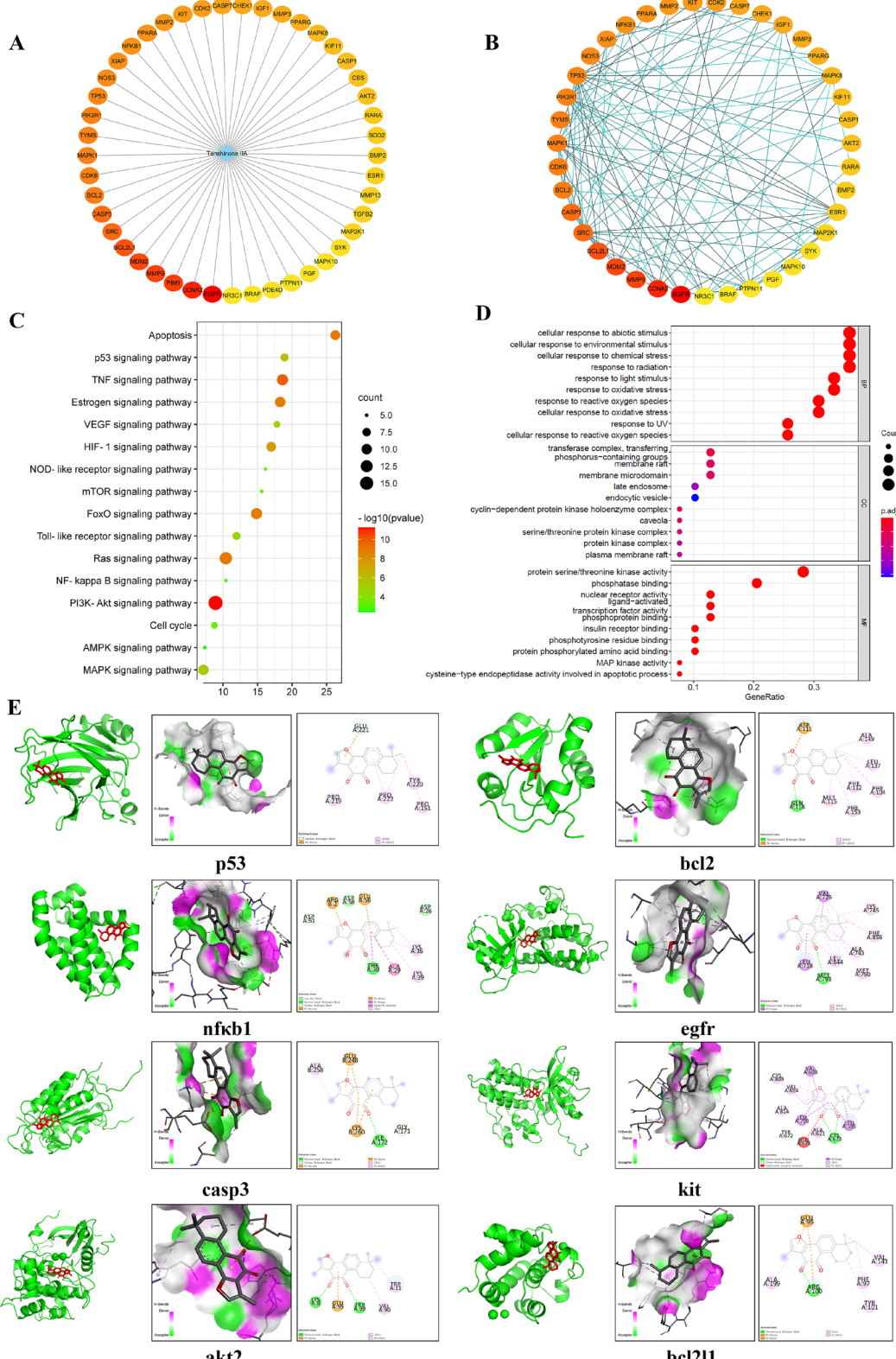


Fig. 4 Network pharmacological analysis of tanshinone IIA. **A** Prediction of Tan II-related targets (the more important the disease target is in triple-negative breast cancer, the redder the color of the node). **B** Protein–protein interaction network (the higher the protein interaction score, the darker the color of the line). **C** Kyoto

Encyclopedia of Genes and Genomes enrichment analysis. **D** Gene Ontology enrichment analysis. **E** Docking exercises of ingredients binding to P53, BCL-2, NF-κB, EGFR, CASP3, KIT, AKT2, and BCL-2L1 (boxes are the 3D and 2D views of the molecular docking domains, respectively)

Table 1 Docking exercises of ingredients binding to p53, Bcl-2, and NF-κB1

Target	Gene ID	PDB ID	Binding energy (kcal/mol)
P53	7157	3D06	-6.92
Bcl-2	596	6GL8	-6.07
NF-κB1	4790	1MDI	-6.28
Egfr	1956	5UG9	-7.88
Casp3	836	4JJE	-5.70
Kit	3815	3G0E	-6.82
Akt2	208	1O6L	-6.40
Bcl-2l1	598	3SP7	-7.07

BCL-2, NF-κB, EGFR, CASP3, KIT, AKT2, and BCL-2L1 are shown in Table 1. Binding affinities to the first three targets were -6.92, -6.07, and -6.28, respectively, indicating a good or strong binding activity. Docking results were visualized in the PyMOL software. Figure 4E shows

Tan IIA docking with P53, BCL-2, NF-κB, EGFR, CASP3, KIT, AKT2, and BCL-2L1, which are mainly related with the cell apoptosis.

Changes in the level of major proteins in Tan IIA-treated 4T1 cells

To investigate the mechanism by which Tan IIA induced apoptosis, Western blotting was utilized to detect Bcl-2, p53, and phosphorylated p53 proteins in 4T1 cells. Western blot results showed that the levels of Bcl-2 gradually reduced in response to increasing Tan IIA concentrations in vitro compared with the control group after Tan IIA treatment ($P < 0.05$ for all, Fig. 5A, B). The levels of p53 and phosphorylated p53 also showed an upward trend. These data showed that Tan IIA could inhibit tumor growth by inducing apoptosis. Taken together, we mapped the hub targets to the canonical signaling pathways according to the results of the network-based systems and molecular-biological analyses. Tan IIA mediated its anti-cancer effects by reducing the

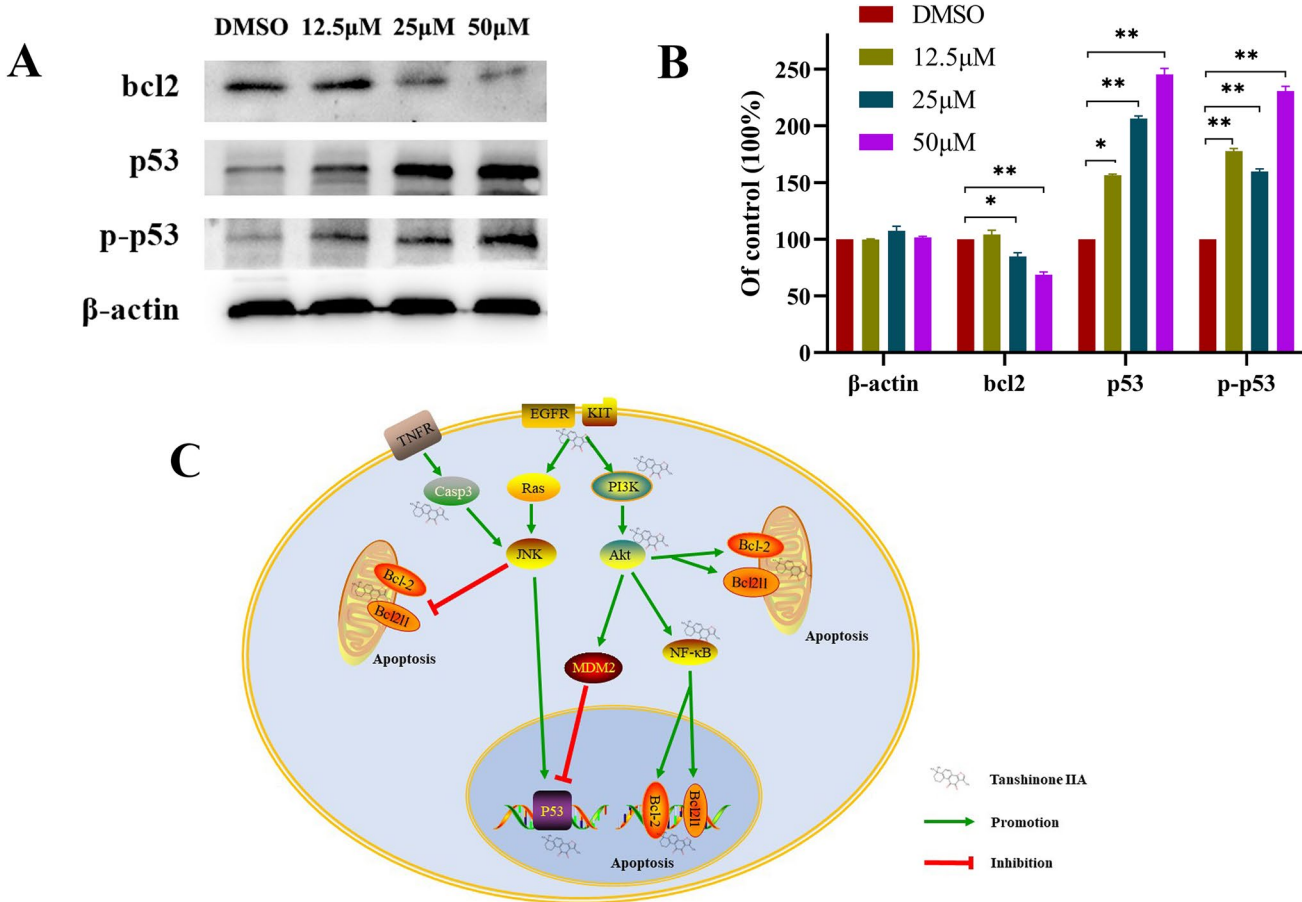


Fig. 5 The changes and mechanisms of target proteins in Tan IIA-treated 4T1 cells. **A, B** Changes in the level of major proteins in Tan IIA-treated 4T1 cells. **C** Potential pro-apoptotic mechanism of Tan IIA. * $P < 0.05$, ** $P < 0.01$

expression of the Bcl-2 and upregulating the expression of P53 through the NF- κ B signaling pathway (Fig. 5C).

Discussion

In recent years, with the in-depth research of bioinformatics, more and more herbal ingredients with anticancer effects have been discovered. Tan IIA, one of the active ingredients of *Salvia miltiorrhiza*, has been demonstrated to have inhibitory effects on multisystem tumors. In human colorectal cancer, Tan IIA effectively inhibits proliferation and metastasis by reducing HIF-1 α levels and inhibiting the secretion of VEGF and bFGF (Sui et al. 2017). Tan IIA enhanced the cell cycle, apoptosis, and autophagy of drug-resistant gastric cancer cells by reducing MRP1, contributing to the anticancer effect of doxorubicin in gastric cancer (Xu et al. 2018). Furthermore, Tan IIA enhanced the sensitivity and pro-apoptotic effects of gefitinib in gefitinib-resistant NSCLC cells by increasing the level of cleaved caspase 3 and downregulating the VEGFR2/Akt pathway (Wang et al. 2019). Multiple in vivo and in vitro experiments have shown that Tan IIA can effectively inhibit the proliferation of TNBC cells, perfecting the evidence that it inhibits the development of various cancers. In the present study, we demonstrated that Tan IIA could significantly suppress the growth of TNBC cells via promoting cell apoptosis. With the bioinformatics detection of Tan IIA, we then found that TP53, NF κ B, AKT, MYC, and BCL2 were the major hub putative targets of Tan IIA. And the apoptotic pathway related to TP53 and BCL2 through pathway cluster analysis may be one of the main mechanisms for the treatment of TNBC.

Cell apoptosis is an important manifestation of cell death, which is strongly associated with tumorigenesis and tumor progression. Bcl-2 is one of the anti-apoptotic proteins, which plays a significant role in mitochondrial-mediated apoptotic pathways. Bcl-2 can inhibit the pro-apoptotic protein Bax (Kale et al. 2018). In addition to playing an important role in regulating cell apoptosis, Bcl-2 can also regulate tumor migration, invasion, autophagy, and angiogenesis (Trisciuoglio et al. 2013). In our experiments, we found Tan IIA could inhibit the 4T1 proliferation and induce the apoptosis by reducing the expression of the Bcl-2. The protein encoded by TP53 responds to diverse cellular stresses to regulate metabolic changes, cell cycle, aging, apoptosis, or DNA repair. In 65–80% of TNBC cases, TP53 is the most commonly mutated gene (Shah et al. 2012). Recent studies have shown that TNBC patients with reduced p53 protein function have a reduced overall survival and an increased risk of metastasis (Powell et al. 2016). There is evidence that if DNA damage stress is strong enough, the phosphorylation of ser46 of

p53 increases, and further induces apoptosis (Taira et al. 2007). According to the predicted results of the network-based systems, p53 was one of the hub targets of Tan IIA for TNBC treatment. Similarly, under the influence of Tan IIA, the expression of TP53 and the phosphorylation of its related sites increased both in vivo and in vitro.

In conclusion, our present results demonstrated that Tan IIA inhibited cell proliferation and tumor growth in vitro and in vivo by inducing cell apoptosis, while the down-regulation of BCL2 and the upregulation of TP53 were the possible mechanisms of Tan IIA in TNBC cell apoptosis. This study further supports the application evidence of Tan IIA in cancer clinical treatment. However, network pharmacological analysis found that the effect of Tan IIA is more than this, and its anticancer mechanism still requires further investigation.

Author contribution JH and XW conceived and designed research. JL, CZ, and SL conducted experiments and wrote the manuscript. XW analyzed data. All authors read and approved the manuscript. The authors declare that all data were generated in-house and that no paper mill was used.

Funding This work was supported by the National Natural Science Foundation of China (Grant No. 81903934) and the National Natural Science Foundation of China (Grant No. 81473441).

Data availability The datasets generated and/or analyzed during the current study are not publicly available due to subsequent experiments that have not been completed but are available from the corresponding author on reasonable request.

Declarations

Ethics approval All experiments were approved by the Experimental Animal Ethics Committee of Nankai University.

Competing interests The authors declare no competing interests.

References

- Arnedos M, Bihan C, Delaloge S, Andre F (2012) Triple-negative breast cancer: are we making headway at least? Ther Adv Med Oncol 4(4):195–210. <https://doi.org/10.1177/1758834012444711>
- Casara P, Davidson J, Claperon A et al (2018) S55746 is a novel orally active BCL-2 selective and potent inhibitor that impairs hematological tumor growth. Oncotarget 9:20075–20088
- Davis AP, Grondin CJ, Johnson RJ et al (2017) The comparative toxicogenomics database: update 2017. Nucleic Acids Res 45:D972–D978
- Davis AP, Wiegers TC, Grondin CJ et al (2020) Leveraging the comparative toxicogenomics database to fill in knowledge gaps for environmental health: a test case for air pollution-induced cardiovascular disease[J]. Toxicol Sci 177(2):392–404
- Gajiwala KS, Wu JC, Christensen J et al (2009) KIT kinase mutants show unique mechanisms of drug resistance to imatinib and

- sunitinib in gastrointestinal stromal tumor patients. *Proc Natl Acad Sci U S A* 106(5):1542–1547
- Hao J, Li SJ (2018) Recent advances in network pharmacology applications in Chinese herbal medicine. *Tradit Med Res* 3(6):260–272
- Hao J, Jin Z, Zhu H et al (2018) Antiestrogenic activity of the Xi-Huang formula for breast cancer by targeting the estrogen receptor α . *Cell Physiol Biochem* 47(6):2199–2215. <https://doi.org/10.1159/000491533>
- Hopkins AL (2008) Network pharmacology: the next paradigm in drug discovery. *Nat Chem Biol* 4(11):682–690. <https://doi.org/10.1038/nchembio.118>
- Jinlong R, Peng L, Jinan W et al (2014) TCMSp: a database of systems pharmacology for drug discovery from herbal medicines[J]. *J Cheminformatics* 6(1):13
- Kale J, Osterlund EJ, Andrews DW (2018) BCL-2 family proteins: changing partners in the dance towards death[J]. *Cell Death Differ* 25(1):65–80
- Li Y, Jiang B, Wang R, Wang J, Li Y, Bao Y (2020) Synergistic effects of tanshinone IIA and andrographolide on the apoptosis of cancer cells via crosstalk between p53 and reactive oxygen species pathways. *Pharmacol Rep* 72(2):400–417. <https://doi.org/10.1007/s43440-019-00006-z>
- Lin C, Wang L, Wang H, Yang L, Guo H, Wang X (2013) Tanshinone IIA inhibits breast cancer stem cells growth in vitro and in vivo through attenuation of IL-6/STAT3/NF- κ B signaling pathways. *J Cell Biochem* 114(9):2061–2070
- Liu Z, Guo F, Wang Y et al (2016) BATMAN-TCM: a bioinformatics analysis tool for molecular mechanism of traditional Chinese medicine[J]. *Sci Rep* 6:21146
- Liu J, Hao J, Niu Y, Wu X (2021) Network pharmacology-based and clinically relevant prediction of active ingredients and potential targets of Chinese herbs on stage IV lung adenocarcinoma patients. *J Cancer Res Clin Oncol* 147(7):2079–2092
- Morris GM, Huey R, Lindstrom W, Sanner MF, Belew RK, Goodsell DS, Olson AJ (2009) (2009) Autodock4 and AutoDockTools4: automated docking with selective receptor flexibility. *J Computational Chemistry* 16:2785–2791
- Planken S, Behenna DC, Nair SK et al (2017) Discovery of N-((3R,4R)-4-fluoro-1-(6-((3-methoxy-1-methyl-1H-pyrazol-4-yl)amino)-9-methyl-9H-purin-2-yl)pyrrolidine-3-yl)acrylamide (PF-06747775) through structure-based drug design: a high affinity irreversible inhibitor targeting oncogenic EGFR mutants with selectivity over wild-type EGFR. *J Med Chem* 60(7):3002–3019
- Powell E, Shao J, Yuan Y et al (2016) p53 deficiency linked to B cell translocation gene 2 (BTG2) loss enhances metastatic potential by promoting tumor growth in primary and metastatic sites in patient-derived xenograft (PDX) models of triple-negative breast cancer[J]. *Breast Cancer Res* 18(1):13
- Qin J, Clore GM, Kennedy WM, Huth JR, Gronenborn AM (1995) Solution structure of human thioredoxin in a mixed disulfide intermediate complex with its target peptide from the transcription factor NF kappa B. *Structure* 3:289–297
- Shah SP, Roth A, Goya R et al (2012) The clonal and mutational evolution spectrum of primary triple-negative breast cancers[J]. *Nature* 486(7403):395–399
- Su CC (2018) Tanshinone IIA can inhibit MiaPaCa-2 human pancreatic cancer cells by dual blockade of the Ras/Raf/MEK/ERK and PI3K/AKT/mTOR pathways. *Oncol Rep* 40(5):3102–3111. <https://doi.org/10.3892/or.2018.6670>
- Suad O, Rozenberg H, Brosh R, Diskin-Posner Y, Kessler N, Shimon LJW, Frolow F, Liran A, Rotter V, Shakhd Z (2009) Structural basis of restoring sequence-specific DNA binding and transactivation to mutant p53 by suppressor mutations. *J Mol Biol* 385:249–265
- Sui H, Zhao J, Zhou L et al (2017) Tanshinone IIA inhibits β -catenin/VEGF-mediated angiogenesis by targeting TGF- β 1 in normoxic and HIF-1 α in hypoxic microenvironments in human colorectal cancer. *Cancer Lett* 403:86–97
- Sung H, Ferlay J, Siegel RL et al (2021) Global cancer statistics 2020: GLOBOCAN estimates of incidence and mortality worldwide for 36 cancers in 185 countries. *CA Cancer J Clin* 71(3):209–249. <https://doi.org/10.3322/caac.21660>
- Szklarczyk D, Franceschini A, Wyder S et al (2014) STRING v10: protein–protein interaction networks, integrated over the tree of life. *Nucleic Acids Res* 43:D447–D452
- Taira N, Nihira K, Yamaguchi T et al (2007) DYRK2 is targeted to the nucleus and controls p53 via Ser46 phosphorylation in the apoptotic response to DNA damage[J]. *Mol Cell* 25(5):725–738
- Trisciuglio D, De Luca T, Desideri M et al (2013) Removal of the BH domain from Bcl-2 protein triggers an autophagic process that impairs tumor growth[J]. *Neoplasia* 15(3):315–327
- Vickers CJ, González-Páez GE, Wolan DW (2013) Selective detection of caspase-3 versus caspase-7 using activity-based probes with key unnatural amino acids. *ACS Chem Biol* 8(7):1558–1566
- Waks AG, Winer EP (2019) Breast cancer treatment: a review. *JAMA* 321(3):288–300. <https://doi.org/10.1001/jama.2018.19323>
- Wang R, Luo Z, Zhang H, Wang T (2019) Tanshinone IIA reverses gefitinib-resistance in human non-small-cell lung cancer via regulation of VEGFR/Akt pathway. *Onco Targets Ther.* 12:9355–9365. <https://doi.org/10.2147/OTT.S221228>
- Wang Y, Zhang S, Li F et al (2020) Therapeutic target database 2020: enriched resource for facilitating research and early development of targeted therapeutics[J]. *Nucleic Acids Res* 48(D1):D1031–D1041
- Wu Q, Zheng K, Huang X, Li L, Mei W (2018) Tanshinone-IIA-based analogues of imidazole alkaloid act as potent inhibitors to block breast cancer invasion and metastasis in vivo. *J Med Chem* 61(23):10488–10501. <https://doi.org/10.1021/acs.jmedchem.8b01018>
- Xian MH, Zhan SK, Zheng KN et al (2021) Neuroprotective effect and mechanism of daidzein in oxygen-glucose deprivation/reperfusion injury based on experimental approaches and network pharmacology. *Tradit Med Res* 6(5):41
- Xu Z, Chen L, Xiao Z et al (2018) Potentiation of the anticancer effect of doxorubicin in drug-resistant gastric cancer cells by tanshinone IIA. *Phytomedicine* 51:58–67. <https://doi.org/10.1016/j.phymed.2018.05.012>
- Xue J, Jin X, Wan X et al (2019) Effects and mechanism of tanshinone II A in proliferation apoptosis and migration of human colon cancer cells. *Med Sci Monit.* 25:4793–4800. <https://doi.org/10.12659/MSM.914446>
- Yang J, Cron P, Good VM, Thompson V, Hemmings BA, Barford D (2002) Crystal structure of an activated Akt/protein kinase B ternary complex with GSK3-peptide and AMP-PNP. *Nat Struct Biol* 9(12):940–944
- Zhou H, Chen J, Meagher JL et al (2012) Design of Bcl-2 and Bcl-xL inhibitors with subnanomolar binding affinities based upon a new scaffold [published correction appears in. *J Med Chem.* 55(10):4664–4682
- Publisher's note** Springer Nature remains neutral with regard to jurisdictional claims in published maps and institutional affiliations.
- Springer Nature or its licensor (e.g. a society or other partner) holds exclusive rights to this article under a publishing agreement with the author(s) or other rightsholder(s); author self-archiving of the accepted manuscript version of this article is solely governed by the terms of such publishing agreement and applicable law.